Velocity dependence of one- and two-electron processes in intermediate-velocity Ar^{16+} + He collisions

W. Wu, J. P. Giese, I. Ben-Itzhak, C. L. Cocke, P. Richard, M. Stockli, R. Ali, and H. Schöne
J. R. Macdonald Laboratory, Department of Physics, Kansas State University, Manhattan, Kansas 66506-2604

R. E. Olson
Physics Department, University of Missouri-Rolla, Rolla, Missouri 65041
(Received 26 May 1993)

We report investigations of one- and two-electron processes in the collisions of 0.9-keV/u to 60-keV/u ($v_p = 0.19-1.55$ a.u.) Ar^{16+} ions with He targets. The cross sections for these processes were measured by observing the final charges of the Ar ions and the recoiling target ions in coincidence. The average Q values for the capture channels were determined by measuring the longitudinal momenta of the recoiling target ions. Single capture (SC) is the dominant process and is relatively independent of the projectile energy. The two-electron transfer-ionization (TI) process is the next largest and slowly increases with projectile energy. The Q values for both SC and TI decrease with increasing projectile energy. Our data thereby suggest that electrons are captured into less tightly bound states as the collision velocity is increased. Both double capture and single ionization are much smaller and fairly independent of the projectile energy. The energy independence of SI is somewhat surprising as our energy range spans the region of the target electron velocity where ionization would be expected to increase. Our analysis suggests that the ionization process is being suppressed by SC and TI processes.

PACS number(s): 34.70.+e, 34.50.Fa

I. INTRODUCTION

One of the fundamental goals of atomic physics is to understand the dynamics of many-electron systems. Such systems are produced in collisions between highly charged ions and many-electron target atoms. The intense fields and large potential energy carried into these collisions by the projectile ions strongly perturb the target. This results in many target electrons being excited, ionized, or transferred to the projectile. The transfer of many electrons to highly charged projectiles often produces multiply excited states not normally found in nature. The study of these collisions therefore offers opportunities to systematically explore the properties of strongly perturbed and unusual many-electron systems.

Collisions of highly charged ions and atoms have been studied extensively at collision velocities either very low [1–5] ($v_p \ll v_e$) or very high [5–7] ($v_p \gg v_e$) compared to the target electrons' average velocities. Charge capture dominates at low velocities where ionization is essentially negligible. Single-electron capture at low velocities is well understood in terms of the formation of molecular orbitals during the collision. Multiple-electron capture is qualitatively understood using either molecular-orbital models or classical overbarrier models. Ionization of the target is the dominant process at high velocities. Ionization and capture at high velocities are both understood in terms of perturbative models.

The intermediate-velocity region ($v_p \sim v_e$) is not as well explored either experimentally or theoretically. These velocities are interesting because capture and ionization processes must be comparable somewhere in this region. Furthermore, neither low-energy molecular-orbital models nor high-energy perturbation models should necessarily be expected to work well at these velocities. Measurements in this region therefore provide a stringent test of our models of both ionization and capture.

Early experiments studying one- and two-electron capture at low velocities measured only the total cross sections [3,4,8]. Most of these experiments used charge-state analysis of the projectile without determining the final recoil charge. Thus, all processes which change the projectile charge by one, for example, single capture and single capture accompanied by additional ionization of the target (transfer ionization or TI), were grouped together. More recent experiments have measured the cross sections as a function of both the projectile and recoil charge states [3,9,10]. This procedure unambiguously determines where all the electrons in the collision system end up. It does not, however, give information on how the electrons reached their final states.

Transfer ionization provides an example of the uncertainty that can arise. At high velocity, the transfer and ionization processes are thought to be independent processes. At low velocity, transfer ionization mainly results from capture into multiply excited states of the projectile. These excited states can autoionize, leaving the projectile with as few as one of the captured electrons. Measuring only the final charges of the projectile and target does not help differentiate between these types of TI and does not provide any direct information on the intermediate, multiply excited state.

Information on the intermediate states can be obtained by measuring additional properties of the reaction products. Experimenters have studied the energy gain [11–13] and scattering angle [3] of the projectile ion,

photon emission [14–16], and electron emission [17–19]. We obtain information on these states using recoil-ion-momentum spectroscopy [20]. The change in electronic energy, or Q value, of a collision process can be calculated from the longitudinal momentum transferred to the recoiling target. The relative population of the intermediate states can in turn be inferred from the Q value.

We have chosen to study the collisions of highly charged Ar^{16+} ions with He atoms. Helium was chosen primarily because it is a simple, two-electron target. The $1s$ ground-state electrons of Ar^{16+} are inactive spectators at our collision velocities, so this collision system is a quasi-two-electron system. Our study is limited to the following processes:

single ionization (SI): $Ar^{16+}+He \rightarrow Ar^{16+}+He^{+}+e^{-}$,

double ionization (DI): $Ar^{16+}+He \rightarrow Ar^{16+}+He^{2+}+2e^{-}$,

single capture (SC): $Ar^{16+}+He \rightarrow Ar^{15+}+He^{+}$,

double capture (DC): $Ar^{16+}+He \rightarrow Ar^{14+}+He^{2+}$,

transfer ionization (TI): $Ar^{16+}+He \rightarrow Ar^{15+}+He^{2+}+e^{-}$.

We present cross sections for all these processes and Q values for the capture processes. Our velocity range (0.19–1.55 a.u.) covers the region around the average velocity of the He electrons (1.34 a.u.), and probes the region of intermediate velocity where the limits of the models of capture and ionization can be tested.

II. EXPERIMENT

We have measured cross sections for these processes by observing the final charges of the Ar ions and recoiling He ions in coincidence. The experimental apparatus is shown in Fig. 1(a) and has been described in detail elsewhere [20]. An Ar^{16+} beam was extracted from the KSU CRYEBIS (cryogenic electron-beam ion source) magnetically analyzed, and accelerated to the collision energy. Charge-state impurities were minimized by cleaning the beam with a magnet immediately prior to the collision region. The angular divergence of the incoming beam was limited to less than 0.01° using adjustable slits and the collision chamber entrance aperture. The collision chamber exit aperture allowed scattering angles up to 2°. After passing through the collision chamber, the projectile ions were charge analyzed by a parallel-plate electrostatic deflector and then detected by a position-sensitive backgammon-anode detector (PSD-1). All three final Ar charge states could be simultaneously observed on this detector. This reduced the uncertainty in the relative cross sections and quickened data collection.

The He gas target was supplied by a multichannel array molecular jet. The gas flow was adjusted to minimize double collisions. As discussed in detail below (see the data analysis section), no more than about 3% of the projectiles that changed their charge state were observed to have undergone double encounters.

The He^{+} and He^{2+} ions produced in the collision region were extracted transverse to the beam by a uniform electric field and detected by a two-dimensional position-sensitive resistive-anode detector (PSD-2). The strength of the recoil extraction field was set high enough (about 60 V/cm) to ensure that all recoil ions were extracted by the field. The recoil charge states were determined by the time-of-flight technique using coincidences between the recoil ions and the projectile ions. The longitudinal recoil momentum was determined from the position of the recoil ions on the detector as discussed below in detail.

III. DATA ANALYSIS

A typical two-dimensional coincidence spectrum and its projections are shown in Fig. 2. The vertical axis represents the position of the projectile ions on PSD-1 and is proportional to the final projectile charge. The horizontal axis represents the time-of-flight (TOF)

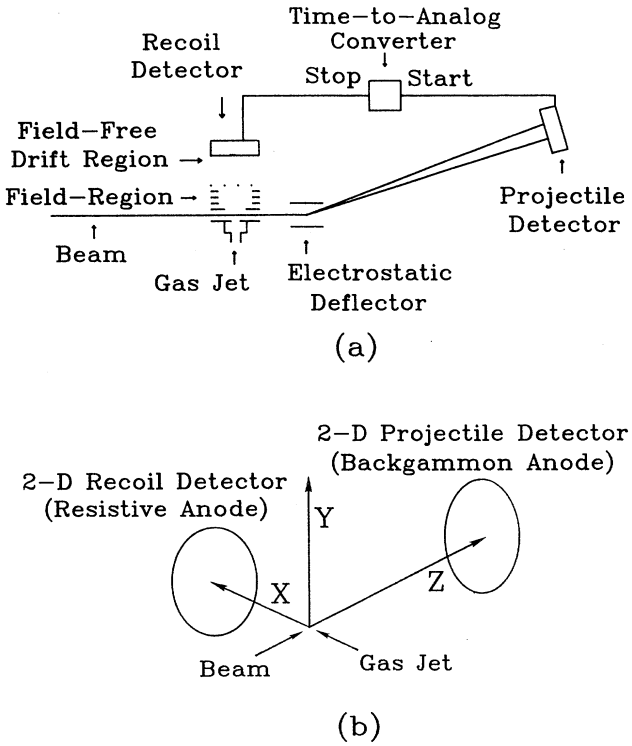

FIG. 1. (a) Schematic of the experimental apparatus and (b) the coordinate system used in the data analysis.

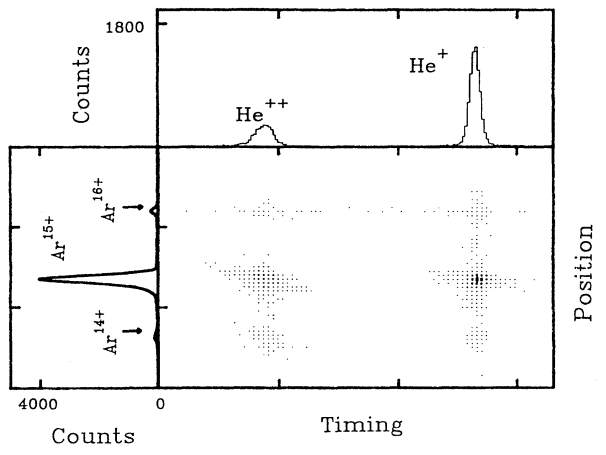

FIG. 2. A typical coincidence spectrum and its projections. The size of the dots in the 2D spectrum is proportional to intensity.

difference between the projectile and recoil ions. The projectile flight times are determined mainly by the initial collision energy and are essentially independent of the final charge. The recoil-ion-flight times are dominated by the energy gained as they are extracted from the collision region and do depend on the final recoil ion charge. The TOF thus identifies the recoil ion charge. Projection onto the TOF axis gives total one- and two-electron loss cross sections for He, while projections onto the position axis give the total single- and double-electron capture cross sections for Ar^{16+}. The cross sections $\sigma_{qq'}^{kk'}$ for the individual processes (SC, TI, etc.) are determined from the corresponding areas of the coincidence spectrum. Here, k and k' denote the initial and final charge states of the recoil ion, and q and q' denote the initial and final charge states of the projectile.

It is necessary to correct the coincidence yields for both random coincidences and events due to multiple collisions. Random coincidences were subtracted by assuming that they are uniformly distributed in the two-dimensional coincidence spectrum. Evidence of double collisions is seen in the yield of Ar^{14+} in coincidence with He^+. It is clearly not possible in one collision for an Ar^{16+} to capture two electrons while a He atom loses only one. Two kinds of double collisions are possible. The first is when an Ar^{16+} captures one electron from either the residual or target gas in the first collision and then ionizes the He target in the second collision. This kind of double collision was negligible for our systems because ionization was always much smaller than capture. The second kind of double collision is when an Ar^{16+} captures two electrons, with one electron captured in each collision. At least one of these capture events must occur in the He target in order to produce a coincidence. A precise measurement of the He target pressure was not possible with our molecular jet. However, we did measure the "double collision" yield as a function of the collision chamber pressure as we varied the He gas flow through the jet. We found that double collisions with one capture in the background gas were one order magnitude smaller than those with both captures in the He target gas itself.

The corrected or "true" coincidence yields ($\mathcal{Y}_{qq'}^{kk'}$) are

$$\mathcal{Y}_{16,16}^{0,1}(\mathrm{SI}) \approx \frac{Y_{16,16}^{0,1}}{1-Y_{16,14}^{0,1}/\mathcal{Y}_{16,15}^{0,1}} ,$$

$$\mathcal{Y}_{16,16}^{0,2}(\mathrm{DI}) \approx \frac{Y_{16,16}^{0,2}}{1-Y_{16,14}^{0,1}/\mathcal{Y}_{16,15}^{0,1}} ,$$

$$\mathcal{Y}_{16,15}^{0,1}(\mathrm{SC}) \approx Y_{16,15}^{0,1}+Y_{16,14}^{0,1} ,$$

$$\mathcal{Y}_{16,15}^{0,2}(\mathrm{TI}) \approx \frac{Y_{16,15}^{0,2}}{1-Y_{16,14}^{0,1}/\mathcal{Y}_{16,15}^{0,1}} ,$$

$$\mathcal{Y}_{16,14}^{0,2}(\mathrm{DC}) \approx \frac{Y_{16,14}^{0,2}-Y_{16,14}^{0,1}\mathcal{Y}_{16,15}^{0,2}/\mathcal{Y}_{16,15}^{0,1}}{1-Y_{16,14}^{0,1}/Y_{16,15}^{0,1}} ,$$

where $Y_{qq'}^{kk'}$ are the coincidence yields after background (random coincidence) subtraction. The corrections for SI, DI, SC, and TI are all due to the loss of the events from these channels caused by double collisions. Consider as an example the case where the projectile has undergone a TI process. If the projectile then captures another electron in a second collision, then the projectile has captured two electrons overall. As a result we lose one real TI event and gain one fake DC event. The corrections for DC are mainly due to these lost TI events. The detailed derivation of these formulas is lengthy and has been described for similar systems in Ref. [6]. The magnitude of the correction is less than 3% for SI, DI, SC, and TI and about 30% for DC.

The relative cross sections were calculated as the ratio of the corrected coincidence yields to the total number of incident projectiles. We normalized our total single-projectile charge change cross section ($\sigma_{16,15}^{0,1}+\sigma_{16,15}^{0,2}$) for 2.3 keV/$q$ Ar^{16+} on He to the same cross section measured by Vancura *et al.* [21]. The measured cross sections for single capture (SC), double capture (DC), single ionization (SI), and transfer ionization (TI) are shown in Fig. 3 as a function of the projectile energy. The error bars shown in the figure account for both statistical errors and reproducibility errors. There is a further uncertainty of 15% in the absolute normalization.

Q values for the capture processes were measured by recoil longitudinal momentum spectroscopy [20]. Conservation of energy and momentum can be used to calculate Q values from the recoil ion momenta as long as no electrons are directly ionized to the continuum . The Q values for collision processes where i electrons are captured are given by

$$Q \approx -v_p P_r^{\parallel} - i\frac{m_e v_p^2}{2} + \frac{m_p+m_r}{2m_p m_r}P_r^{\perp 2} + \frac{1}{2m_r}P_r^{\parallel 2} ,$$

where E_0 is the initial projectile kinetic energy, $v_p=\sqrt{2E_0/m_p}$ is the projectile velocity, m_p, m_r, and m_e are the masses of the projectile, target, and electron, respectively, and $P_r^{\parallel}$ and $P_r^{\perp}$ are components of the recoil momentum longitudinal and transverse to the beam direction. The transverse recoil momentum is generally much greater than the longitudinal momentum for our

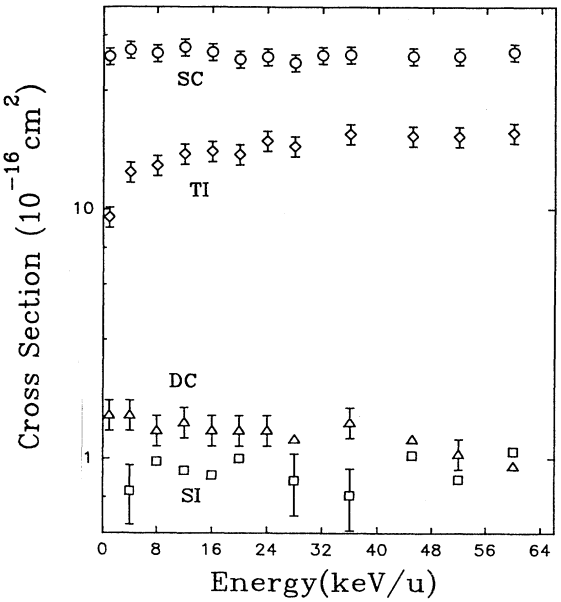

FIG. 3. Measured cross sections for Ar^{16+} on He. Circles, SC; diamonds, TI; triangles, DC; squares, SI. Some typical error bars are shown.

collision system and energies. However, because the projectile velocity, v_p, is much larger than $v_r^{\perp}=P_r^{\perp}/m_r$, the first two terms dominate the Q value. We measured the transverse recoil ion momenta from the widths of the corresponding TOF peaks [22]. The results show that the contribution of the transverse momentum to the Q value is less than 1%.

The longitudinal momenta of the recoil ions was determined from the longitudinal component of their positions on PSD-2 and from their times of flight. The zero point corresponding to zero longitudinal momentum must be determined in order to measure the average shift of the recoil ions due to their longitudinal momentum. We did this by measuring the times-of-flight and recoil ion positions at different extraction fields. These data were then fitted using the kinematic relation:

$$z = z_0 - \frac{P_r^{\parallel}}{m_r} t \ .$$

The coordinates used are shown in Fig. 1(b), with z describing the recoil position along the beam direction, z_0 the zero point, t the recoil ion time-of-flight, and $P_r^{\parallel}$ the longitudinal recoil momentum. The displacement of the centroid of the recoil ion position from z_0 was then used to determine the average longitudinal recoil momentum.

The average Q values for SC and TI are plotted in Fig. 4. The Q values for TI were calculated by assuming that TI is mostly autoionizing DC. The Q-value error bars are due mainly to uncertainty in locating both the centroid of the recoil-ion-position spectra and the zero of the recoil position.

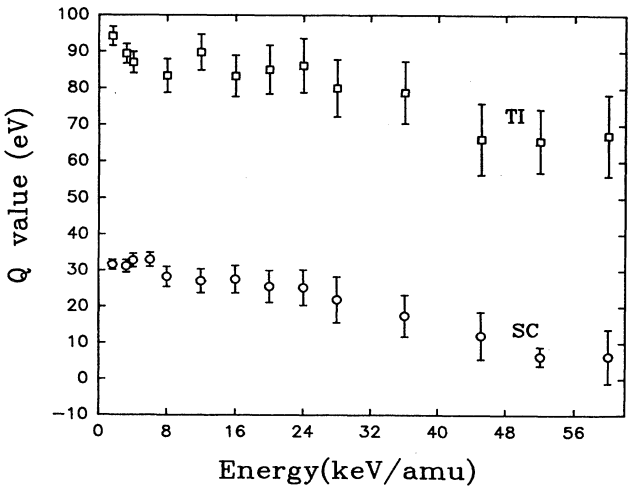

FIG. 4. The measured Q values for SC (circles) and TI (squares).

IV. RESULTS AND DISCUSSION

A. Single capture

The one-electron, single-capture process is the most likely process at all of our collision energies. The SC cross sections are relatively large and fairly independent of energy. Good estimates of the approximate principal quantum number of the captured electron can be obtained from the classical overbarrier model (CBM) [23]. This velocity-independent model predicts that $n=7.3$ for Ar^{16+} on He. This estimate seems reasonable as the measured cross section is in agreement with the CBM prediction of 49×10^{-16} cm^2.

The velocity independence of our SC cross sections can be understood in terms of simple models. According to the molecular-orbital (MO) model, capture occurs at localized crossings of the initial and final electronic states. When the projectile is highly charged, many of these crossings can be active, i.e., there is a range of states to which the capture reaction can occur. The cross section depends in part on the number of possible final states within this "reaction window." As the collision velocity is increased, the reaction window moves toward smaller internuclear radii and capture proceeds to more tightly bound states. The density of final states around $n=7$ is fairly uniform for Ar^{15+}. Therefore, as the velocity increases and the reaction window moves, there are always about the same number of crossings in the window. As a result, the total cross section is insensitive to the collision velocity. Our SC cross sections suggest that this simple model of SC works up to velocities over 1.55 a.u. It should be noted that the velocity independence of our SC cross sections qualitatively agrees with detailed calculations for total single capture in the one-electron systems of bare projectiles on atomic hydrogen [24,25].

The puzzle is that the general MO model predicts that the Q value for this collision system would be either relatively energy independent or would slowly *increase* as the projectile velocity increased. Note that the MO prediction is consistent with measurements and calculations us-

ing very fast projectiles, which produce capture to more tightly bound states (i.e., larger Q values) as the velocity is increased. Both the low-velocity MO model and the high-velocity perturbative models directly contradict our data (see Fig. 4). We have calculated the average final projectile n state from the measured Q values by assuming H-like states with a core charge of 16. The electrons seem to be captured into about $n=8$ orbitals at lower energy and about $n=11$ orbitals at higher energy.

Other measurements and calculations show no consistent dependence of the final n state on velocity. Some authors [13,26] reported a general tendency of capture to smaller n with increasing velocity, while others [14,18,27,28] reported a tendency to larger n. These investigations were at somewhat lower velocities ($v<0.6$ a.u.) and used projectiles of much lower charge states ($q\leq 8$) than the ones used in our experiment. A direct comparison between these different collision systems with our system therefore may not be enlightening. However, these results suggest that the velocity dependence of the projectile state population may be sensitive to the properties of the individual collision systems.

There are presently no detailed quantum or semiclassical calculations available which give the n-state populations for capture by such highly charged projectiles in this velocity region. At these relatively high velocities and large impact parameters, it is possible that the classical trajectory Monte Carlo (CTMC) model could give reasonable results. We have used the nCTMC method where both electrons are explicitly included [29] to calculate both the recoil longitudinal momenta ($P_r^{\parallel}$) and the cross sections as a function of the final n state of the captured electron. The CTMC total single-capture cross section agrees with the data in both its energy independence and magnitude. The calculated $P_r^{\parallel}$ and Q values also reproduce both the magnitude and the energy dependence of the data fairly well [Figs. 5(a) and 5(b)]. However, the general slope of the energy dependence is steeper for the data than for calculations. Note that at very high energies, the CTMC calculation suggests that $P_r^{\parallel}$, and therefore the Q value, increases with energy [Fig. 5(c)]. This indicates capture into more tightly bound states as would be expected by high-velocity, perturbative models.

We attempt to test the validity of the CTMC model at this relatively low velocity region by comparing its results for single capture in the collision system O^5+H with the atomic-orbital expansion calculations done by Tawara and Fritsch [30]. The predictions of the cross section as a function of n for the two models are shown in Fig. 6. The agreement is excellent for projectile energies above 35 keV/u. The deviations below about 25 keV/u suggest that quantum effects are becoming more important at lower velocities. Note that both models indicate that while the n value of the peak of the reaction window for capture is relatively insensitive to velocity, the width of the reaction window is increasing with velocity. This broadening seems to be mainly towards higher n and should therefore lead to smaller average Q values. The O^{5+} projectiles used for this comparison have a much lower charge than the Ar ions used in the experiment.

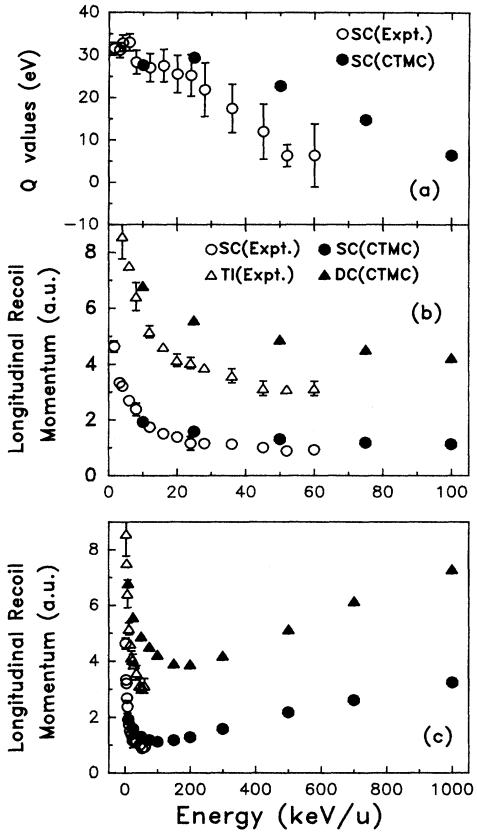

FIG. 5. A comparison of Q values (a) and recoil longitudinal momenta (b) and (c) from the data (open symbols) and the nCTMC calculations (closed symbols). The circles represent SC, while the triangles represent TI for the data and DC for the calculation. Note that the TI observed at these energies is thought to result from DC followed by autoionization, hence the comparison of our TI data with the CTMC calculation.

This validity test can therefore only suggest that the CTMC results are reasonable.

The CTMC calculation demonstrates that capture to higher n states as velocity increases is possible in some systems. We believe the fundamental cause of this trend is the kinetic energy carried into the collision by the target electron. Our SC cross sections are relatively constant, suggesting that the average distance at which capture occurs is fairly constant. The potential energy of the captured electron relative to the projectile at the moment of capture must also be fairly constant. The electron's kinetic energy relative to the projectile, however, increases with the square of the collision velocity. The CTMC model explicitly accounts for this kinetic energy and therefore can reproduce the velocity dependence of the measured Q values. MO models can also account for this kinetic energy by using electron translational factors [1,2]. Our data and CTMC calculations suggest that there is a range of intermediate collision velocities where this kinetic energy strongly affects the final-state populations.

A related explanation of our result can be made based on experiments [14,3] and calculations [27,30] which

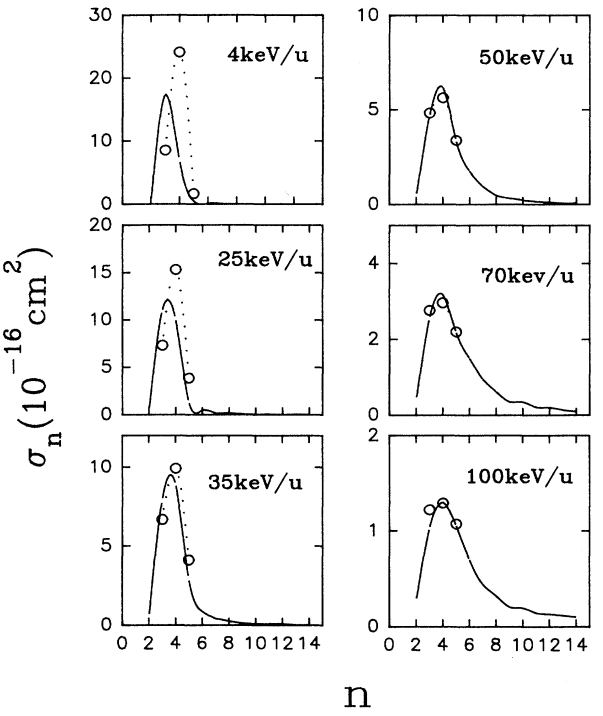

FIG. 6. $O^{5+}+H$ single-capture cross sections as a function of n. Solid line: CTMC; circle and dotted line: atomic orbital expansion.

have shown the tendency of electrons to be captured to higher angular momentum states (l states) with increasing velocity. We know that electrons captured by highly charged ions end up in high n states, where the density of states is high and fairly uniform. If there is a strong propensity to capture into high l states with increasing velocity, then a simple phase-space argument would suggest that the electron should be captured to higher n states.

B. Transfer ionization and double capture

Transfer ionization is the second most likely process at all our collision energies as is seen in Fig. 3. Transfer ionization by slow, highly charged ions colliding with He is generally thought to occur when the projectile captures both electrons into doubly excited states [3]. These states can decay by either autoionization, leading to TI, or by radiative stabilization, leading to "true" double capture. Note from Fig. 3 that DC is about an order of magnitude smaller than TI in this collision system. Our measured Q values for TI and DC are the same, suggesting both that our TI cross section is dominated by autoionizing double capture and that the same range of doubly excited states are populated in each process. Using the average Q values for TI, the final states of the captured electrons were estimated to be $(n,n')=(6,7)$ and (7,7) at the lower energy. The decreasing Q value suggests that the relative population of (7,7) slowly increases with increasing projectile energy. The measured recoil longitudinal momenta for TI are compared to the calculated values for DC in Fig. 5(b) and have about the same magnitude and energy dependence. This further suggests that the measured TI is a product of autoionizing DC. Note, however, that the difference in the slopes between the data and calculation is larger for these two-electron processes than that was for SC.

The ratio of true double capture to all two-electron capture events, $\sigma_{DC}/(\sigma_{TI}+\sigma_{DC})$, is plotted in Fig. 7 and decreases with increasing collision energy. If our TI is really autoionizing double capture, this ratio gives an average fluorescence yield for the populated doubly excited states. Calculations of the decay rates for these Ar^{14+} doubly excited states [31] indicate that a shift from (6,7) to (7,7) can explain the observed decrease in this ratio. Note that a shift from (6,7) to (7,7) can explain the decrease in both the measured average Q values and fluorescence yields. Our data therefore consistently suggest that the two-electron DC and TI processes, like the one-electron SC process, populate more highly excited states as the projectile velocity is increased.

C. Single ionization

Single ionization is the least likely process at all our collision energies except the very highest, where it approaches DC in magnitude. Electron capture by metastables in the Ar^{16+} beam may mimic ionization when the resulting doubly excited Ar^{15+} undergoes autoionization. However, the metastable contamination of beams produced in the CRYEBIS is negligible due to the long contaminant time relative to the lifetime of the Ar^{16+} ($1s2s\ ^3S_1$) state (0.21 μs). Double ionization was negligibly small at all our collision energies.

The mere observation of SI at these energies is not surprising because it has been previously observed at even lower energies [32,33] for highly charged projectiles. The relative energy independence of the single ionization, however, was surprising to us because we expected the ionization to begin increasing in the region around matching velocity (45 keV/u). Our expectations were based in part on simple models of ionization which often do not consider the competing process of capture. However, even coupled-channel calculations of bare projec-

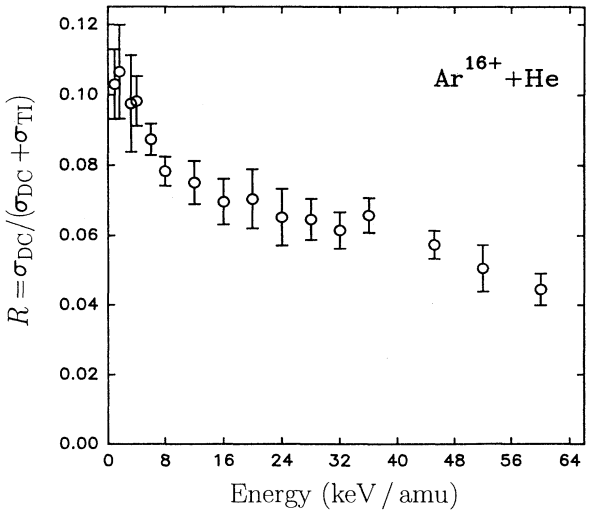

FIG. 7. The ratio of $\sigma_{DC}/(\sigma_{DC}+\sigma_{TI})$ as a function of projectile energy.

tiles on H which did attempt to account for both ionization and capture show a rapidly increasing ionization cross section in the velocity range covered by our data [25,34]. We have developed a model which includes the interplay between capture and ionization around the matching velocity and which does help explain the energy independence of single ionization.

One should in principle treat the two-target electron as a whole and compute the probabilities of the competing processes of capture, ionization, or remaining on the target consistently using one model. Our simple model including both capture and ionization, however, was developed within the independent electron approximation [35–38]. The cross sections for the different processes are given by

$$\sigma_{SC}=2\pi\int_0^\infty 2P_c(b)Rb\,db\ ,$$

$$\sigma_{DC}=2\pi\int_0^\infty P_c^2(b)b\,db\ ,$$

$$\sigma_{SI}=2\pi\int_0^\infty 2P_i(b)Rb\,db\ ,$$

$$\sigma_{TI}=2\pi\int_0^\infty 2P_i(b)P_c(b)b\,db\ ,$$

where $P_c(b)$ and $P_i(b)$ are the capture and ionization probabilities per active electron, and $R(b)=1-P_c(b)-P_i(b)$ is the probability for the spectator electron to remain on the He target. We have used the classical overbarrier model to describe capture and the semiclassical Coulomb approximation (SCA) to describe ionization. The two target electrons are treated as equivalent electrons, i.e., in two-electron processes we have neglected effects due to the increase in binding energy of the second electron. Such treatment is not rigorously correct and will tend to overestimate the two-electron processes. However, this treatment is computationally easier and does provide qualitative insight into the collision mechanism.

The CBM capture probability is a constant for impact parameters smaller than the capture radius, which is about $R_c=10$ a.u. for $Ar^{16+}+He$ collisions, and zero otherwise. The value of this constant, $P_c(b)=0.4$, was evaluated using the measured SC cross section. This $P_c(b)$ has a sharp cutoff at R_c which is not physical. We remove this sharp cutoff using a functional form suggested by Brandt [39] which takes into account the time the electron spends within the capture radius. The capture probability is then given by $P_c(b)=P_0\sqrt{1-b^2/R_c^2}$, where $P_0=0.5$ and $R_c=12$ were evaluated using the measured values of the SC and DC cross sections. None of the calculated cross sections were sensitive to the smoothing of this cutoff.

The ionization probabilities were obtained from the SCA tables of Hansteen, Johansen, and Kocbach [40]. This approximation is probably good for this collision system at large impact parameters where $P_i(b)$ is small. However, it overestimates $P_i(b)$ at small impact parameters where perturbation theory is not valid for the large-q^2 scaling factor needed for the Ar^{16+}. As a result, $P_c^{CBM}(b)<P_i^{SCA}(b)$ and $P_c^{CBM}(b)+P_i^{SCA}(b)>1$ for small impact parameters. We know that SC is dominant over SI in our systems, so we have defined the ionization probability as the complement of the capture probability at small impact parameters, i.e., $P_i(b)=1-P_c(b)$ and $R(b)=0$, wherever $P_c^{CBM}(b)+P_i^{SCA}(b)\geq 1$.

The probabilities $P_c(b)$, $P_i(b)$, and $R(b)$ are shown in Fig. 8 for $E_p=50$ keV/u. It can be seen that below about $b_0=3$ a.u. the ionization probability is suppressed by the competing capture probability and the probability of retaining the electron on the He target is practically zero. The value of b_0 increases slowly with increasing energy.

The calculated and measured cross sections are shown in Fig. 9 and are in reasonable agreement over the entire energy range. As was mentioned in Sec. IV B above, the measured TI is probably due to autoionizing double capture. The TI and DC channels were therefore summed into one cross section labeled as DC+TI in this comparison. The calculated SI cross section increases only very slowly with increasing collision velocity. The large increase expected around matching velocity is suppressed by the competing capture process. We expect that SI will increase more rapidly only at higher collision energies where SC begins to decrease with energy.

It is of special interest to see at what range of impact parameters each of these processes peaks. The probability functions of all these processes multiplied by b are plotted as a function of b in Fig. 10. SC is the dominant process at large impact parameters. The two-electron processes are dominant for close collisions where it is unlikely that either electron will remain on the He target. Interestingly, single-ionization peaks at intermediate impact parameters of ~4 a.u. This exclusive process is suppressed at small b by the requirement that one electron has to remain on the target and at large b by the

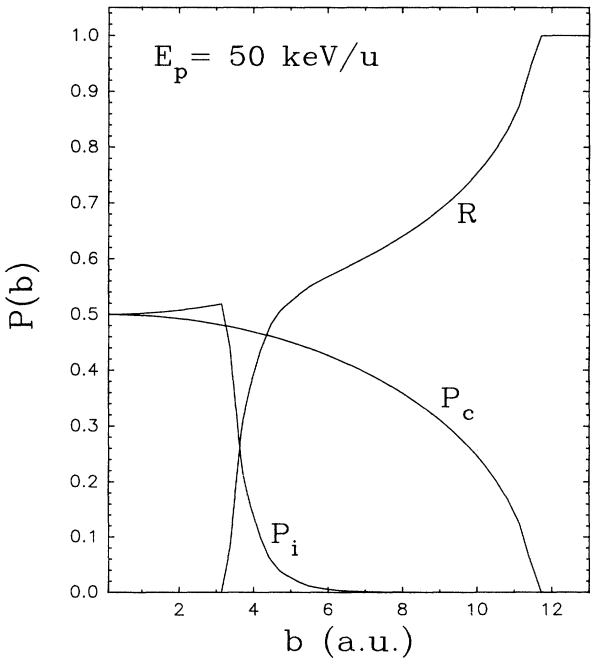

FIG. 8. Probabilities for electron capture (P_C), ionization (P_i), and remaining on the He target (R), as a function of the impact parameter for $E=50$ keV/u.

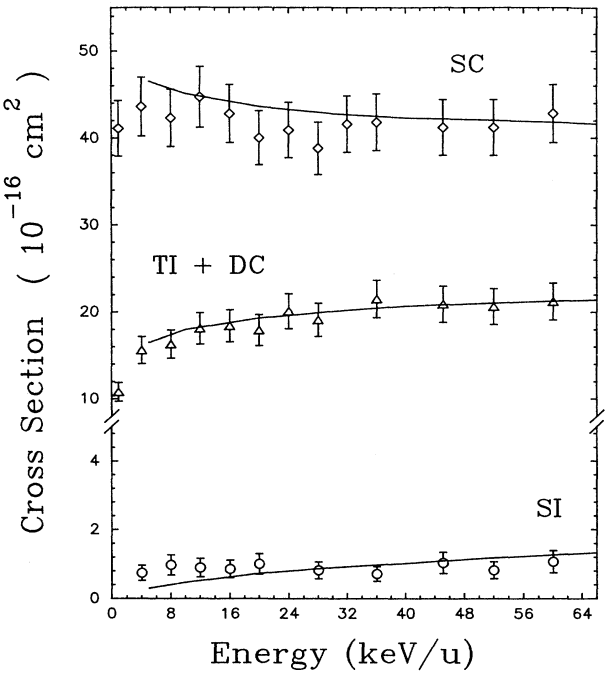

FIG. 9. A comparison of the total cross sections for single capture (SC), single ionization (SI), and double capture + transfer ionization (DC+TI) from the data (open symbols) and our IEM calculation (continuous lines).

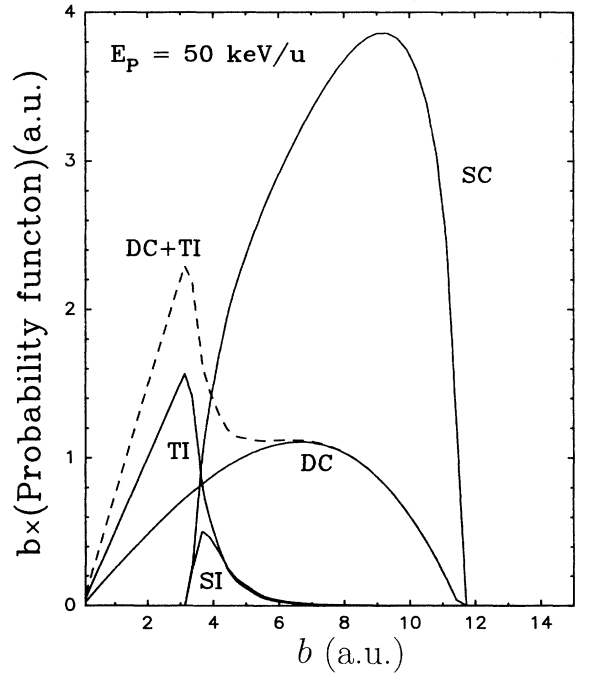

FIG. 10. Probability functions multiplied by b for single capture (SC), single ionization (SI), double capture (DC), and transfer ionization (TI), as a function of the impact parameter. Note that in this calculation TI is "real" TI , i.e., independent capture and ionization of two electrons, while in the data TI is thought to be autoionizing DC.

capture process which dominates due to the large electron-projectile attraction. At very large parameters where capture is negligible the ionization probabilities are also negligible.

The maximum in the ionization probability function at intermediate impact parameters disagrees with the known behavior in fast collisions for which ionization is dominant at large impact parameters (soft collisions) while capture is dominant for small impact parameters [41]. This behavior in fast collisions is easily explained by our model as the capture probability is negligible except at very small impact parameters and never suppresses the ionization probability.

The prediction of our simple model that SI might only occur at intermediate impact parameters can also be understood in terms of MO models. We have plotted the Coulomb potential energy curves as a function of the internuclear distance, R in Fig. 11. The SC and DC channels cross the initial $Ar^{16+}+He$ potential energy curve at $R_C(1)$ and $R_C(2)$, respectively. The DC channel then crosses the SI curve at much smaller impact parameters around $R_c(3)$. Note that SI can occur only via crossings with these capture processes at internuclear radii smaller than about 3 a.u. These radii are quite similar to the radii predicted for SI in Fig. 10 by our independent-electron model. These potential energy curves suggest that SI of He by these slow, highly charged ions might also be thought of as a two-electron process, whereby the two electrons are first transferred to the projectile ending up on the DC potential curve. When the projectile penetrates closer to the He nucleus one of those electrons is ejected into the continuum while the other falls back onto the target He. Although this picture seems to have somewhat different physical content from our simple independent-electron model, it does also point to ionization at intermediate impact parameters and the two pictures might not be incomparable.

We should note that ionization by very highly charged Xe ions ($q > 30$) incident on Xe targets has been recently observed at very low velocities ($v = 0.034\sqrt{q}$ a.u.) [32,33]. These results are explained in terms of the formation of core-excited, autoionizing, neutral target states. It is proposed that a target electron is first cap-

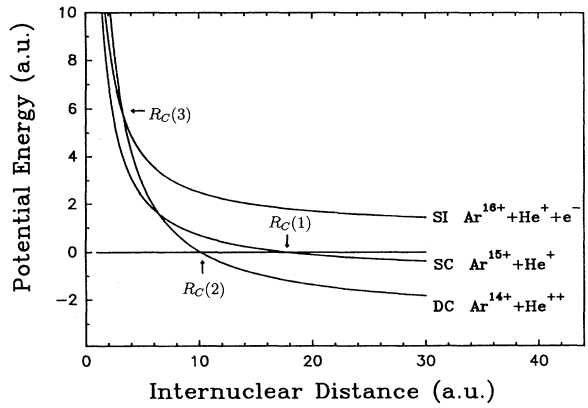

FIG. 11. Potential-energy curves as a function of the internuclear distance for the $Ar^{16+}+He$ system.

tured by the projectile at a MO crossing at relatively large internuclear distances. As the projectile and target move closer together, the electron is then transferred back to the target via a MO crossing between the single-capture orbital and the core-excited target state. Although this model depends on the $3p^6$ structure of the target Xe, it is in principle very similar to the model of ionization via successive promotion along MO crossings at intermediate internuclear distances discussed before. The study of ionization by highly charged ions at low and intermediate velocities offers the opportunity for detailed study of this process.

V. CONCLUSION

Our studies of one- and two-electron processes in collisions of Ar^{16+} with He have produced two interesting and somewhat surprising results. First, our measurements of the Q values for SC and TI suggest that both one- and two-electron capture proceed to less tightly bound states as the projectile energy is increased. This result suggests that the collisional kinetic energy of the captured electron strong affects the final-state populations. Second, our SI cross sections were small and relatively independent of collision energy. This is surprising as our energy range spans the region where SI is expected to rapidly increase. We developed a model which suggests this behavior results from suppression of SI by SC at large impact parameters and by two-electron processes at small impact parameters.

ACKNOWLEDGMENTS

We express our thanks to Dr. Luzheng Meng and Dr. N. Toshima for their help in performing some of the calculations. This work was supported by the Division of Chemical Sciences, Office of Basic Energy Sciences, Office of Energy Research, U.S. Department of Energy.

[1] R. K. Janev and L. P. Presnyakov, Phys. Rep. **70**, 1 (1981).
[2] R. K. Janev and H. Winter, Phys. Rep. **117**, 265 (1985).
[3] M. Barat and P. Roncin, J. Phys. B **25**, 2205 (1992).
[4] T. Iwai, Y. Kaneko, M. Kimula, N. Kobayashi, S. Ohtani, K. Okuno, S. Takagi, H. Tawara, and S. Tsurubuchi, Phys. Rev. A **26**, 105 (1982).
[5] H. Knudsen, H. K. Haugen, and P. Hvelplund, Phys. Rev. A **23**, 597 (1981).
[6] J. L. Shinpaugh, J. M. Sanders, J. M. Hall, D. H. Lee, H. Schmit-Böcking, T. N. Tipping, T. J. M. Zouros, and P. Richard, Phys. Rev. A **45**, 2922 (1992).
[7] R. Hippler, S. Datz, P. D. MIller, P. L. Pepmiller, and P. F. Dittner, Phys. Rev. A **35**, 585 (1987).
[8] A. Müller, H. Klinger, and E. Salzborn, Phys. Lett. **55A**, 11 (1975).
[9] C. L. Cocke, R. DuBois, T. J. Gray, E. Justiniano, and C. Can, Phys. Rev. Lett. **46**, 1671 (1981).
[10] A. Müller, W. Groh, and E. Salzborn, Phys. Rev. Lett. **51**, 107 (1983).
[11] O. Okuno, H. Tawara, T. Iwai, Y. Kaneko, M. Kimura, N. Kobayashi, A. Matsumoto, S. Ohtani, S. Takayi, and S. Tsurubuchi, Phys. Rev. A **28**, 127 (1983).
[12] C. Schemissner, C. L. Cocke, R. Mann, and W. E. Meyerhoh, Phys. Rev. A **30**, 1661 (1984).
[13] M. Barat, M. N. Gaboriand, L. Guillement, P. Roncin, H. Laurent, and S. Andriamonje, J. Phys. B **20**, 577 (1987).
[14] D. Dijkkamp, C. Ćirić, E. Vlieg, A. de Boer, and F. J. de Heer, J. Phys. B **18**, 4763 (1985).
[15] S. Martin, Y. Ouardane, A. Denis, and M. Carre, Z. Phys. D **21**, S277 (1991).
[16] J. P. M. Beijers, R. Hoekstra, A. R. Schlatmann, R. Morgenstern, and F. J. de Heer, J. Phys. B **25**, 463 (1992).
[17] A. Bordenave-Montesquieu, P. Benoit-Cattin, M. Bondjema, A. Gleizes, S. Dousson, and D. Hitz, J. Phys. B **17**, L127 (1984).
[18] P. Moretto-Cappelle, P. Benoit-Cattin, A. Bordenave-Montesquieu, and A. Gleizes, Z. Phys. D **21**, S283 (1991).
[19] M. Mack, J. H. Nijlang, P. Van de Straten, A. Niehaus, and R. Morgenstern, Phys. Rev. A **39**, 3846 (1989).
[20] R. Ali, V. Frohne, C. L. Cocke, M. Stockli, S. Cheng, and M. L. A. Raphaelian, Phys. Rev. Lett. **69**, 2491 (1992).
[21] J. Vancura, V. J. Marchetti, J. J. Perotti, and V. O. Kostroun, Phys. Rev. A **47**, 3758 (1993).
[22] J. C. Levin, R. T. Short, C.-S. O, H. Cederquist, S. B. Elston, J. P. Gibbons, I. A. Sellin, and H. Schmidt-Böcking, Phys. Rev. A **36**, 1649 (1987).
[23] H. Ryufuku, K. Sasaki, and T. Watanabe, Phys. Rev. A **21**, 745 (1980).
[24] R. E. Olson and A. Salop, Phys. Rev. A **16**, 531 (1977).
[25] H. Ryufuku, Phys. Rev. A **25**, 720 (1982).
[26] C. Harel and H. Jouin, J. Phys. B **25**, 221 (1992).
[27] C. Harel and H. Jouin, J. Phys. B **21**, 859 (1988).
[28] W. Fritsch and C. D. Lin, J. Phys. B **19**, 2683 (1986).
[29] R. E. Olson, J. Ulrich, and H. Schmidt-Böcking, Phys. Rev. A **39**, 5572 (1989).
[30] H. Tawara and W. Fritsch, Phys. Scr. **T28**, 58 (1989).
[31] J. E. Hansen, J. Phys. (Paris) Colloq. **50**, C1-603 (1989).
[32] H. Cederquist, H. Anderson, E. Beebe, C. Biedermann, L. Borström, Å Engström, H. Gao, R. Hutton, J. C. Levin, M. Pajek, T. Quinteros, N. Selberg, and P. Sigray, in *Proceedings of the Seventeenth International Conference on the Physics of Electronic and Atomic Collisions, Brisbana, Australia, 1991,* edited by W. R. MacGilliuvay, I. E. McCarthy, and M. C. Standage (AIP, New York, 1992), p. 391.
[33] H. Cederquist, C. Biedermann, N. Selberg, E. Bebbe, M. Pajek, and A. Barany, Phys. Rev. A **47**, R4551 (1993).
[34] R. K. Janev and L. P. Presnyakov, J. Phys. B **13**, 4233 (1980).
[35] J. H. McGuire and O. L. Weaver, Phys. Rev. A **16**, 41 (1977).
[36] R. E. Olson, J. Phys. B **11**, 1843 (1979).
[37] W. E. Meyerhof, R. Anholt, Xiang-Yuan Xu, H. Gould, B. Felsberg, R. J. McDonald, H. E. Wegner, and P. Thieberger, Nucl. Instrum. Methods Phys. Res., Sect. A **262**, 10 (1987).
[38] I. Ben-Itzhak, T. J. Gray, J. C. Legg, and J. H. McGuire, Phys. Rev. A **37**, 3685 (1988).
[39] D. Brandt, Nucl. Instrum. Methods **214**, 93 (1983).
[40] J. H. Hansteen, O. M. Johansen, and L. Kocbach, At. Data Nucl. Data Tables **15**, 305 (1975).
[41] T. J. Gray, C. L. Cocke, and E. Justiniano, Phys. Rev. A **22**, 849 (1980).